Speed Control of a Five-Phase Induction Motor Drive using Modified Super-Twisting Algorithm

Y. Kali[1], J. Rodas[2], M. Saad[3], R. Gregor[2], K. Benjelloun[1], J. Doval-Gandoy[4] and G. Goodwin[5]
[1]Engineering School, École Mohammadia d'Ingénieurs, University of Mohammed V, Morocco (y.kali88@gmail.com)
[2]Laboratory of Power and Control Systems, Facultad de Ingeniería, Universidad Nacional de Asunción, Paraguay
[3]Department of Electrical Engineering, École Technologie Supérieure, Canada
[4]Applied Power Electronics Technology Research Group, Universidad de Vigo, Spain
[5]School of Electrical Engineering and Computer Science, University of Newcastle, Australia

***Abstract*—Field oriented control, with an outer speed loop and inner current loops, has been the most common control strategy for multiphase drives. For the inner current control, the proportional-integral pulse-width modulation and finite-control-set model predictive control have been the most analyzed implementations. The present work proposes an alternative for the inner current control based on the modified super-twisting algorithm with time delay estimation. Simulation results were carried out to verify the performance of the proposed robust control strategy for a five-phase induction motor drive. A stability analysis is also presented.**

***Index Terms*—Super-twisting algorithm, time delay estimation, multiphase induction machine, speed control, current control, field oriented control.**

I. Introduction

Multiphase drives have been selected as a real competitor of the traditional three-phase drives for high-power and reliable applications such as wind energy generation systems and electric vehicles [1]–[3]. Most of the control strategies applied for multiphase drives are an extension of the three-phase case such as proportional-integral pulse-width modulation (PI-PWM), proportional-resonant (PR), finite-control-set model predictive control (FCS-MPC), predictive torque control (PTC), direct torque control (DTC), sensorless, among others [4]–[10]. Recent works also extends the above-mentioned techniques to the post-fault operation [11]–[14]. However, little attention has been paid to robust controllers based on fuzzy logic or sliding mode control (SMC) strategies [15].

Nowadays, SMC is one of the robust proposed nonlinear controllers based on high gain switching controller that forces the system trajectory to converge to a user-chosen surface [16]. However, to ensure robustness, the switching gain should be larger than uncertainties that are assumed to be bounded. Therefore, the choice of an excessive switching gain causes the well-known chattering phenomenon [17], [18]. This phenomenon has a negative impact on the actuators of the system and can deteriorate the controlled systems if the control has a physical sense.

To overcome this phenomenon, the most famous proposed method is higher order sliding mode (HOSM) [19], [20]. Since introduced, many algorithms have been proposed to improve the HOSM control such as twisting algorithm, sub-optimal algorithm, global algorithm, super-twisting algorithm (STA) and others [20]–[22]. However, all these algorithms except STA, increase the required measurements which make the implementation difficult. The STA has provided good results [23], [24] without a prior knowledge of the values of the state derivatives. However, this technique requires the knowledge of the uncertainties. These bounds are overestimated which make the choice of the gains too large.

Motivated to deal with all these problems, this work proposes a combination of STA and time delay estimation (TDE) [25]. Although, TDE has a very simple structure, its effectiveness has been demonstrated through many applications [26], [27]. TDE provides an estimation of uncertainties and disturbances by observing the inputs and the states of the system one step into the past while STA will be used to ensure finite-time convergence of the sliding surface to zero and to reduce chattering.

In this paper, STA with TDE is proposed for the inner current control loop of a rotor field oriented control (RFOC) of a five-phase induction motor (IM) drive. The rest of the paper is organized as follows. Section II presents the mathematical model of the system while controller design is explained in Section III. Simulation results are provided in Section IV. Section V draws some conclusions.

II. Mathematical Model of Five-phase IM

The considered system consists of a symmetrical five-phase IM drive fed by a five-phase converter as depicted in Fig. 1. Its mathematical model can be found in [6]. This continuous-time system can be defined by a set of differential equations given by:

$$\dot{X}_1(t) = A_1X_1(t) + H_1X_3(t) + B_1U_1(t) \tag{1}$$

$$\dot{X}_2(t) = A_2X_2(t) + B_2U_2(t) \tag{2}$$

$$\dot{X}_3(t) = A_3X_1(t) + H_3X_3(t) + B_3U_1(t) \tag{3}$$

$$Y(t) = [X_1(t), X_2(t)]^T. \tag{4}$$

The stator i_s and rotor i_r currents are selected as state variables in the $\alpha - \beta$ and $x - y$ sub-spaces as follows: $X_1(t) = [i_{s\alpha}, i_{s\beta}]^T$, $X_2(t) = [i_{sx}, i_{sy}]^T$ and $X_3(t) = [i_{r\alpha}, i_{r\beta}]^T$. The stator voltages are the input vectors defined as: $U_1(t) = [u_{s\alpha}, u_{s\beta}]^T$ and $U_2(t) = [u_{sx}, u_{sy}]^T$ while the rest of matrices are defined as follows:

$$A_1 = \begin{bmatrix} -R_s \frac{L_r}{L_s L_r - M^2} & M \frac{M}{L_s L_r - M^2} \omega_r \\ -M \frac{M}{L_s L_r - M^2} \omega_r & -R_s \frac{L_r}{L_s L_r - M^2} \end{bmatrix} \quad (5)$$

$$H_1 = \begin{bmatrix} R_r \frac{M}{L_s L_r - M^2} & L_r \frac{M}{L_s L_r - M^2} \omega_r \\ -L_r \frac{M}{L_s L_r - M^2} \omega_r & R_r \frac{M}{L_s L_r - M^2} \end{bmatrix} \quad (6)$$

$$A_2 = \begin{bmatrix} -R_s \frac{1}{L_{ls}} & 0 \\ 0 & -R_s \frac{1}{L_{ls}} \end{bmatrix} \quad (7)$$

$$A_3 = \begin{bmatrix} R_s \frac{M}{L_s L_r - M^2} & -M \frac{L_s}{L_s L_r - M^2} \omega_r \\ M \frac{L_s}{L_s L_r - M^2} \omega_r & R_s \frac{M}{L_s L_r - M^2} \end{bmatrix} \quad (8)$$

$$H_3 = \begin{bmatrix} -R_r \frac{L_s}{L_s L_r - M^2} & -L_r \frac{L_s}{L_s L_r - M^2} \omega_r \\ L_r \frac{L_s}{L_s L_r - M^2} \omega_r & -R_r \frac{L_s}{L_s L_r - M^2} \end{bmatrix} \quad (9)$$

$$B_1 = \begin{bmatrix} \frac{L_r}{L_s L_r - M^2} & 0 \\ 0 & \frac{L_r}{L_s L_r - M^2} \end{bmatrix} \quad (10)$$

$$B_2 = \begin{bmatrix} \frac{1}{L_{ls}} & 0 \\ 0 & \frac{1}{L_{ls}} \end{bmatrix} \quad (11)$$

$$B_3 = \begin{bmatrix} -\frac{M}{L_s L_r - M^2} & 0 \\ 0 & -\frac{M}{L_s L_r - M^2} \end{bmatrix} \quad (12)$$

where R_s and R_r are the stator and rotor resistances, respectively. The inductances are represented by $L_s = L_{ls} + 3\, L_m$ for the stator and $L_r = L_{lr} + 3\, L_m$ for the rotor being L_{ls} and L_{lr} the stator and rotor leakage inductances, L_m the magnetizing inductance and M is the mutual inductance. The rotor electrical speed ω_r and the rotor mechanical speed ω_m are related $\omega_r = p\, \omega_m$, being p the number of pole pairs. The following Clarke matrix T_1 is used to convert the phase variables in the $\alpha-\beta$, $x-y$ and z sub-spaces with $\vartheta = 2\pi/5$:

$$T_1 = \frac{2}{5} \begin{bmatrix} 1 & \cos(\vartheta) & \cos(2\vartheta) & \cos(3\vartheta) & \cos(4\vartheta) \\ 0 & \sin(\vartheta) & \sin(2\vartheta) & \sin(3\vartheta) & \sin(4\vartheta) \\ 1 & \cos(2\vartheta) & \cos(4\vartheta) & \cos(\vartheta) & \cos(3\vartheta) \\ 0 & \sin(2\vartheta) & \sin(4\vartheta) & \sin(\vartheta) & \sin(3\vartheta) \\ \frac{1}{2} & \frac{1}{2} & \frac{1}{2} & \frac{1}{2} & \frac{1}{2} \end{bmatrix}. \quad (13)$$

The generated electromagnetic torque is related to $\alpha-\beta$ sub-space as shown in the following equation:

$$T_e = \frac{5}{2} p\, M\, (i_{r\beta} i_{s\alpha} - i_{r\alpha} i_{s\beta}) \quad (14)$$

while the $x-y$ components are related to the copper losses. The rotor electrical speed has a relationship with torque as follows:

$$J_m\, \dot{\omega}_r + B_m\, \omega_r = p\, (T_e - T_L) \quad (15)$$

being B_m and J_m the friction and the inertia coefficient, respectively, and T_L the load torque.

Then, by using another transformation matrix T_2 the $\alpha-\beta$ sub-space components are transformed in the dynamic components $d-q$:

$$T_2 = \begin{bmatrix} \cos(\delta_r) & -\sin(\delta_r) \\ \sin(\delta_r) & \cos(\delta_r) \end{bmatrix} \quad (16)$$

where δ_r is the rotor angular position referred to the stator.

III. Controller Design

A. Outer Control Loop

The aim of the outer loop is to control the speed. To that end, a PI controller with a saturator is used due to its simplicity. For the outer loop, the PI speed controller is selected to obtain the dynamic reference current i^*_{qs}. Then, the process of the slip frequency (ω_{sl}) estimation is executed in the same way as the indirect RFOC methods, from the reference currents (i^*_{ds}, i^*_{qs}) in the dynamic reference frame and the electrical parameters of the five-phase IM.

B. Inner Control Loop

The aim of the inner loop is to control the stator currents. To that end, in the first part, a modified STA will be designed to force the stator current in the $\alpha-\beta$ sub-space to converge to their desired references in finite-time with high accuracy even in presence of unmeasurable states (i,e. rotor currents). In the second part, the classical STA will be used to control the stator current in the $x-y$ sub-space due to its simplicity, its robustness and its finite-time convergence.

1) Control of Stator Current in $\alpha-\beta$ Sub-Space: To quantify the control objective, let $X_1^d(t) = i^*_{s\phi}(t) \in R^2$ to be the desired trajectory with $\phi \in \{\alpha, \beta\}$ and $e_\phi(t) = X_1(t) - X_1^d(t) = i_{s\phi}(t) - i^*_{s\phi}(t) \in R^2$ be the tracking error. Now, let us select the sliding surface [16] to be the error variable as:

$$\sigma_\phi(t) = e_\phi(t). \quad (17)$$

Then, the time derivative of $\sigma_\phi(t)$ is calculated as follows:

$$\begin{aligned} \dot{\sigma}_\phi(t) &= \dot{e}_\phi(t) = \dot{X}_1(t) - \dot{X}_1^d(t) \\ &= A_1 X_1(t) + H_1 X_3(t) + B_1 U_1(t) - \dot{X}_1^d(t). \end{aligned} \quad (18)$$

The standard form of STA in [28] is expressed as:

$$\begin{aligned} \dot{\sigma}_\phi(t) &= -\Gamma_1 \Lambda(\sigma_\phi(t)) \operatorname{sign}(\sigma_\phi(t)) + \xi(t) \\ \dot{\xi}(t) &= -\Gamma_2 \operatorname{sign}(\sigma_\phi(t)) \end{aligned} \quad (19)$$

where $\Lambda(\sigma_\phi(t)) = \operatorname{diag}\big(|\sigma_{\phi,1}(t)|^{0.5}, |\sigma_{\phi,2}(t)|^{0.5}\big)$, $\Gamma_1 = \operatorname{diag}(\Gamma_{11}, \Gamma_{12})$ and $\Gamma_2 = \operatorname{diag}(\Gamma_{21}, \Gamma_{22})$ are diagonal positive matrices where the coefficients will be fixed later and $\operatorname{sign}(\sigma_\phi(t)) = [\operatorname{sign}(\sigma_{\phi,1}(t)), \operatorname{sign}(\sigma_{\phi,2}(t))]^T$ with:

$$\operatorname{sign}(\sigma_{\phi,i}(t)) = \begin{cases} 1, & \text{if } \sigma_{\phi,i}(t) > 0 \\ 0, & \text{if } \sigma_{\phi,i}(t) = 0 \\ -1, & \text{if } \sigma_{\phi,i}(t) < 0 \end{cases} \quad (20)$$

By resolving (19) using (18), the control input is obtained as:

$$\begin{aligned} U_1(t) = &-B_1^{-1} \left[A_1 X_1(t) + H_1 X_3(t) - \dot{X}_1^d(t)\right] \\ &+ B_1^{-1} \left[-\Gamma_1 \Lambda(\sigma_\phi(t)) \operatorname{sign}(\sigma_\phi(t)) + \xi(t)\right]. \end{aligned} \quad (21)$$

Since the states $X_3(t)$ are not measurable, the control performance will be affected. Then, assuming that the unmeasurable states are slow varying during a small L period of time, $X_3(t)$ can be estimated using TDE method [25], [27] as:

$$\hat{X}_3(t) = H_1^{-1} \left[\dot{X}_1(t-L) - A_1 X_1(t-L) - B_1 U_1(t-L)\right] \quad (22)$$

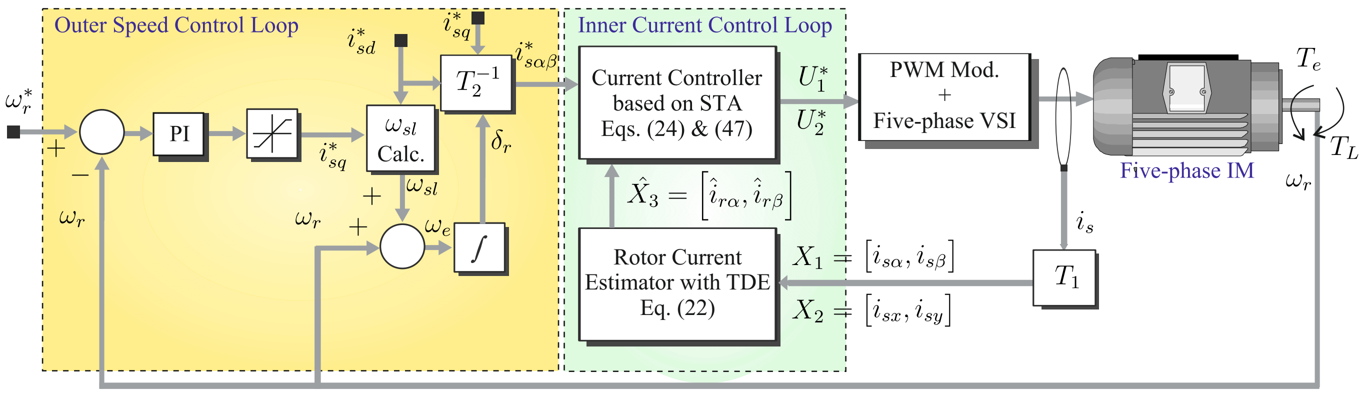

Fig. 1. Block diagram of the proposed speed control based on RFOC technique and the modified STA for the inner current control.

where L is the estimation time delay. Clearly the accuracy of $\hat{X}_3(t)$ improves as L decreases. In practice, the smallest possible value of L is the sampling time period. The time delayed $\dot{X}_1(t-L)$ can be obtained by the following approximation:

$$\dot{X}_1(t-L) = \frac{1}{L}\left[X_1(t-L) - X_1(t-2L)\right] \tag{23}$$

Theorem 3.1: The proposed modified STA for the stator current in $\alpha - \beta$ sub-space (1) is given by:

$$\begin{aligned} U_1(t) &= U_1(t-L) - B_1^{-1}A_1\left(X_1(t) - X_1(t-L)\right) \\ &\quad - B_1^{-1}\left[\dot{X}_1(t-L) - \dot{X}_1^d(t) - \xi(t)\right] \\ &\quad - B_1^{-1}\Gamma_1\Lambda(\sigma_\phi(t))\,\mathrm{sign}(\sigma_\phi(t)) \end{aligned} \tag{24}$$

where the gains Γ_{1i} and Γ_{2i} for $i = 1, 2$ satisfy:

$$\Gamma_{1i} > 2, \quad \Gamma_{2i} > \frac{\Gamma_{1i}^3 + 4\delta_i^2(\Gamma_{1i} - 2)}{4(\Gamma_{1i}^2 - 2\Gamma_{1i})} \tag{25}$$

with $\delta_i > 0$. In addition, the proposed controller ensures the convergence of the sliding surface $\sigma_\phi(t)$ to zero in a finite-time T_c smaller than:

$$T_{c,\max} = 2\frac{\sqrt{\lambda_{\max}\{P\}}}{\lambda_{\min}\{Q\}}V^{\frac{1}{2}}(\eta(0)) \tag{26}$$

Proof. Substituting the calculated control input in (24) in the stator current system (1) leads to:

$$\begin{aligned} \dot{\sigma}_\phi(t) &= -\Gamma_1\Lambda(\sigma_\phi(t))\,\mathrm{sign}(\sigma_\phi(t)) + \xi(t) \\ \dot{\xi}(t) &= -\Gamma_2\,\mathrm{sign}(\sigma_\phi(t)) + \dot{\varepsilon}(t) \end{aligned} \tag{27}$$

where $\varepsilon(t) = H_1[X_3(t) - \hat{X}_3(t)]$ is the TDE error. Now, let us decompose the above closed-loop error dynamics into 2 sub-systems as:

$$\begin{aligned} \dot{\sigma}_{\phi,i}(t) &= -\Gamma_{1i}|\sigma_{\phi,i}(t)|^{0.5}\,\mathrm{sign}(\sigma_{\phi,i}(t)) + \xi_i(t) \\ \dot{\xi}_i(t) &= -\Gamma_{2i}\,\mathrm{sign}(\sigma_{\phi,i}(t)) + \dot{\varepsilon}_i(t). \end{aligned} \tag{28}$$

Then, for the stability analysis, the following Lyapunov function in quadratic form is selected [28]:

$$V(t) = \eta^T(t)P\eta(t) \tag{29}$$

where $\eta(t) = [\eta_{1i}(t) \quad \eta_{2i}(t)]^T$ with $\eta_{1i}(t) = |\sigma_{\phi,i}(t)|^{0.5}\mathrm{sign}(\sigma_{\phi,i}(t))$ and $\eta_{2i}(t) = \xi_i(t)$ and P is a positive definite symmetric matrix. Except at $\sigma_{\phi,i} = 0$, the selected Lyapunov function is continuous and differentiable, definite positive and radially bounded by choosing P as:

$$P = \frac{1}{2}\begin{bmatrix} \Gamma_{1i}^2 + 4\Gamma_{2i} & -\Gamma_{1i} \\ -\Gamma_{1i} & 2 \end{bmatrix} \tag{30}$$

One has:

$$\lambda_{\min}\{P\}\|\eta(t)\|_2^2 \leq V(t) \leq \lambda_{\max}\{P\}\|\eta(t)\|_2^2 \tag{31}$$

with $\lambda_{\min}\{P\}$ and $\lambda_{\max}\{P\}$ denote respectively the minimum and maximum eigenvalues of P and $\|\eta(t)\|_2^2$ is the Euclidean norm of $\eta(t)$. Therefore, the time derivative of $V(t)$ is calculated as:

$$\dot{V}(t) = \dot{\eta}^T(t)P\eta(t) + \eta^T(t)P\dot{\eta}(t) \tag{32}$$

where $\dot{\eta}(t) = [\dot{\eta}_{1i}(t), \dot{\eta}_{2i}(t)]^T$ with:

$$\dot{\eta}_{1i}(t) = \frac{1}{2|\sigma_{\phi,i}(t)|^{0.5}}\dot{\sigma}_{\phi,i}(t), \quad \text{and} \quad \dot{\eta}_{2i}(t) = \dot{\xi}_i(t). \tag{33}$$

Notice that $|\eta_{1i}(t)| = |\sigma_{\phi,i}(t)|^{0.5}$. Then, $\dot{\eta}(t)$ is given by:

$$\dot{\eta}(t) = \frac{1}{|\eta_{1i}(t)|}\left(A\eta(t) + B\dot{\varepsilon}_i(t)|\eta_{1i}(t)|\right) \tag{34}$$

where:

$$A = \begin{bmatrix} -\frac{1}{2}\Gamma_{1i} & \frac{1}{2} \\ -\Gamma_{2i} & 0 \end{bmatrix}, \quad B = \begin{bmatrix} 0 \\ 1 \end{bmatrix} \tag{35}$$

Substituting $\dot{\eta}(t)$ in $\dot{V}(t)$ leads to:

$$\begin{aligned} \dot{V}(t) &= \frac{1}{|\eta_{1i}(t)|}\eta^T(t)\left(A^TP + PA\right)\eta(t) \\ &\quad + \frac{2\dot{\varepsilon}_i(t)}{|\eta_{1i}(t)|}|\eta_{1i}(t)|B^TP\eta(t). \end{aligned} \tag{36}$$

Otherwise, assuming that the time derivative of TDE error is bounded $|\dot{\varepsilon}_i(t)| \leq \delta_i$ with $\delta_i > 0$. Then:

$$\begin{aligned} & 2\dot{\varepsilon}_i(t)|\eta_{1i}(t)|B^TP\eta(t) \\ & \leq \dot{\varepsilon}_i^2(t)|\eta_{1i}(t)|^2 + \eta^T(t)PBB^TP\eta(t) \\ & \leq \delta_i^2\eta^T(t)C^TC\eta(t) + \eta^T(t)PBB^TP\eta(t) \end{aligned} \tag{37}$$

where $C = [1\ 0]$. Finally, using (36) and (37), one has:

$$\dot{V}(t) \leq -\frac{1}{|\eta_{1i}(t)|}\eta^T(t)Q\eta(t) \tag{38}$$

where Q is calculated as follows:

$$\begin{aligned} Q &= -(A^T P + PA + \delta_i^2 C^T C + PBB^T P) \\ &= \begin{bmatrix} \frac{1}{2}\Gamma_{1i}^3 - \frac{1}{4}\Gamma_{1i}^2 + \Gamma_{1i}\Gamma_{2i} - \delta_i^2 & \star \\ -\frac{1}{2}(\Gamma_{1i}^2 - \Gamma_{1i}) & \frac{1}{2}\Gamma_{1i} - 1 \end{bmatrix} \end{aligned} \tag{39}$$

where $\star = -\frac{1}{2}(\Gamma_{1i}^2 - \Gamma_{1i})$. Using the gains in (25), the conditions given in [29] are held:

$$\frac{1}{2}\Gamma_{1i} - 1 > 0, \quad \det(Q) > 0 \tag{40}$$

As the conditions above are held, the obtained Q is symmetrical positive definite. Therefore, $\dot{V}(t)$ is negative definite. Then:

$$\dot{V}(t) \leq -\frac{1}{|\eta_{1i}(t)|}\lambda_{\min}\{Q\}\|\eta(t)\|_2^2 \tag{41}$$

where $\lambda_{\min}\{Q\}$ is the minimum eigenvalue of Q. From this above analysis, the stability of the closed-loop is proven.

Now, let us recall (31) and (38) to prove the finite-time convergence. In a first part, using (31) gives:

$$\frac{V^{\frac{1}{2}}(t)}{\lambda_{\max}^{\frac{1}{2}}\{P\}} \leq \|\eta(t)\|_2 \leq \frac{V^{\frac{1}{2}}(t)}{\lambda_{\min}^{\frac{1}{2}}\{P\}} \tag{42}$$

In the other part, as $|\eta_{1i}(t)| \leq \|\eta(t)\|_2$, so using (38) and the above equation gives:

$$\dot{V}(t) \leq -\frac{1}{\|\eta(t)\|_2}\lambda_{\min}\{Q\}\|\eta(t)\|_2^2 \leq -\frac{\lambda_{\min}\{Q\}}{\lambda_{\max}^{\frac{1}{2}}\{P\}}V^{\frac{1}{2}}(t) \tag{43}$$

According to the equation above, the maximum convergence time of the sliding surface can be set as in (26). This concludes the proof.

2) Control of Stator Current in $x-y$ Sub-Space: A complete study of classical STA theory can be found in [28]. In this section, a brief presentation of its basic theory to control the stator current in the $x-y$ sub-space will be given. The sliding surface here is selected as:

$$\sigma_{xy}(t) = e_{xy}(t) = X_2(t) - X_2^d(t) \tag{44}$$

where $X_2^d(t) = [i_{sx}^*(t),\ i_{sy}^*(t)]^T$ denotes the desired currents and $e_{xy}(t)$ represents the tracking error. Therefore, the time derivative of $\sigma_{xy}(t)$ is:

$$\begin{aligned} \dot{\sigma}_{xy}(t) &= \dot{e}_{xy}(t) = \dot{X}_2(t) - \dot{X}_2^d(t) \\ &= A_2 X_2(t) + B_2 U_2(t) - \dot{X}_2^d(t) \end{aligned} \tag{45}$$

The expression of the classical STA [28] is given by:

$$\begin{aligned} \dot{\sigma}_{xy}(t) &= -K_1\Lambda(\sigma_{xy}(t))\,\mathrm{sign}(\sigma_{xy}(t)) + \pi(t) \\ \dot{\pi}(t) &= -K_2\,\mathrm{sign}(\sigma_{xy}(t)) \end{aligned} \tag{46}$$

where $\Lambda(\sigma_{xy}(t)) = \mathrm{diag}\big(|\sigma_x(t)|^{0.5}, |\sigma_y(t)|^{0.5}\big)$, $K_1 = \mathrm{diag}(k_{11}, k_{12})$ and $K_2 = \mathrm{diag}(k_{21}, k_{22})$ are diagonal positive matrices and $\mathrm{sign}(\sigma_{xy}(t)) = [\mathrm{sign}(\sigma_x(t)), \mathrm{sign}(\sigma_y(t))]^T$.

Then, the control input is obtained by resolving (46) using (45).

Theorem 3.2: The classical STA for the stator current in the $x-y$ sub-space (2) is given by:

$$\begin{aligned} U_2(t) = &-B_2^{-1}\left[A_2 X_2(t) - \dot{X}_2^d(t) + \pi(t)\right] \\ &- B_2^{-1}K_1\Lambda(\sigma_{xy}(t))\,\mathrm{sign}(\sigma_{xy}(t)) \end{aligned} \tag{47}$$

Moreover, all current trajectories converge in finite-time to their desired references, in a time smaller than:

$$T_{c1,\max} = \frac{2V^{\frac{1}{2}}(0)}{\gamma} \tag{48}$$

where γ is a constant depending on the gains K_1 and K_2.

Proof. Refer to [28].

IV. Numerical Simulation

A MATLAB/Simulink simulation program has been designed for a five-phase IM in order to prove the effectiveness of the proposed modified STA. Numerical integration using first order Euler's discretization method has been applied to compute the evolution of the state space variables in the time domain. The electrical and mechanical parameters of the five-phase IM are detailed in Table I.

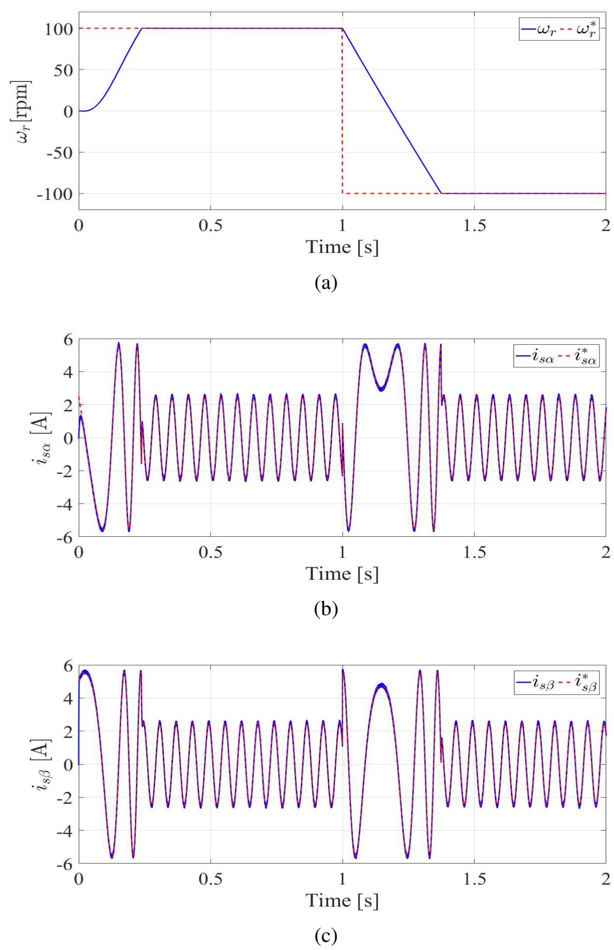

Fig. 2. Simulation results for a fixed speed reference ω_r^* of 100 rpm and a reversal Speed tracking condition (a) ω_r tracking, (b) $i_{s\alpha}$ tracking and (c) $i_{s\beta}$ tracking.

TABLE I
ELECTRICAL AND MECHANICAL PARAMETERS OF THE FIVE-PHASE IM

PARAMETER	VALUE	PARAMETER	VALUE
R_r (Ω)	6.77	M (mH)	656.5
R_s (Ω)	19.45	Nominal Speed (rpm)	1 000
L_{lr} (mH)	100.7	Nominal Power (kW)	1
L_{ls} (mH)	38.06	p	3
B_m (Nms/rad)	0.0221	J_m (Kg-m^2)	0.109

In this simulation, a sampling frequency of 10 kHz, a torque load of 2 Nm when $\omega_r = 100$ rpm and 0 Nm when $\omega_r = -100$ rpm and a fixed d current ($i^*_{ds} = 2.5$ A) have been used. The PI gains are chosen to be $K_p = 9.18$ and $K_I = 0.27$. In addition, the gains of the modified STA used for stator currents tracking in $\alpha - \beta$ sub-space are:

$$\Gamma_1 = \text{diag}(15, 15), \;\; \Gamma_2 = \text{diag}(3, 3)$$

While the gains of the STA used for stator currents tracking in $x - y$ sub-space are:

$$K_1 = \text{diag}(10, 10), \;\; K_2 = \text{diag}(2, 2)$$

The behavior of the stator currents in the $\alpha - \beta$ and $x - y$ sub-spaces are shown in Fig. 2 and Fig. 3, respectively. The controllers used ensures high accuracy tracking of the system currents to their desired references in a finite-time. In the case of the stator currents in the $\alpha - \beta$ sub-space, this is thanks to a good estimation of the unmeasurable rotor currents and disturbances.

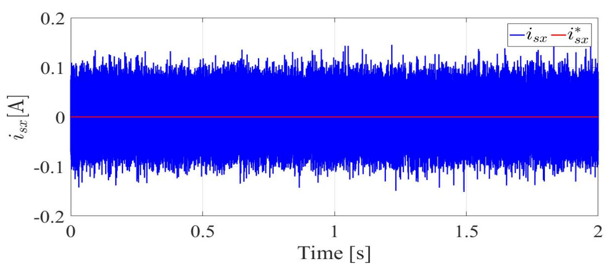

(a)

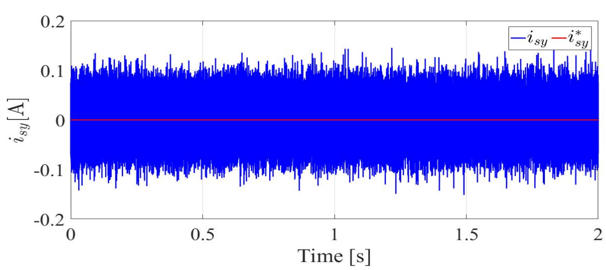

(b)

Fig. 3. Simulation results of $x - y$ stator currents and their references: (a) i_{sx} and tracking and (b) i_{sy} tracking.

Then, the simulation results of the dynamic performance using the proposed method are shown in Fig. 4. In this test, the q stator current reference i^*_{qs} is varying according to a step profile. The measured $d - q$ stator currents follow with high accuracy their desired references, which confirms that the proposed controller works well at different mechanical speed and during transient states.

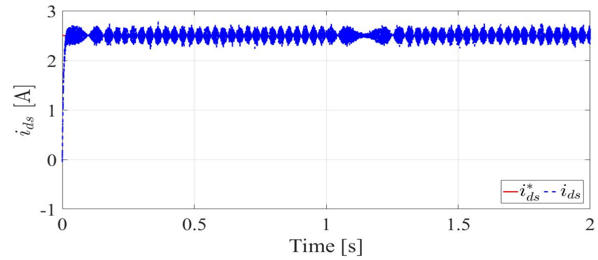

(a)

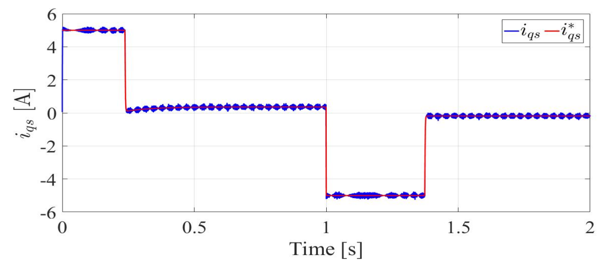

(b)

Fig. 4. Simulation results of $d - q$ currents and their references: (a) i_{ds} and tracking and (b) i_{qs} tracking.

Furthermore, it can be seen that the control inputs in the $\alpha - \beta$ are smooth and the chattering phenomenon is reduced as depicted in Fig. 5.

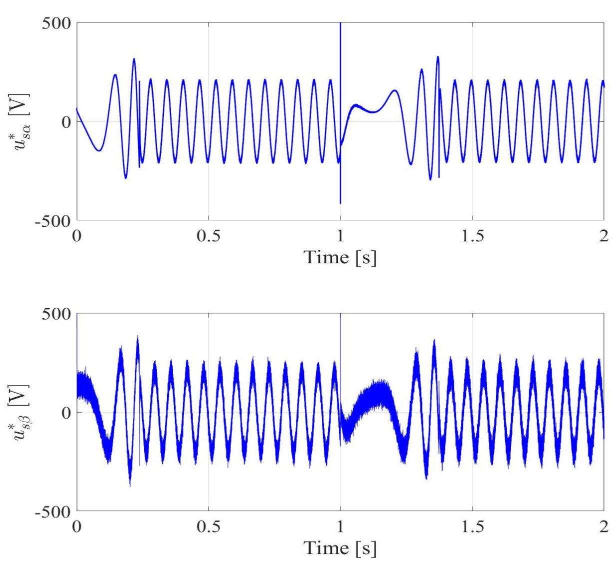

Fig. 5. Simulation results of control input reference in the $\alpha - \beta$ sub-space.

V. CONCLUSION

In this paper, a speed control based on RFOC strategy with an inner STA with TDE current control is proposed. One of the main advantages of the proposed method is that the unmeasurable currents are estimated simply and effectively using TDE method while the STA provides smooth control inputs and eliminates the hard nonlinearities caused by TDE error. The efficiency of the proposed method is confirmed by numerical simulations. The proposed controller provides excellent performances in steady state as well as in dynamic process. Furthermore, the average switching frequency of the proposed method is even lower than the conventional SMC and other controllers. Further research will be initiated for real-time implementation and for the extension of the theoretical part to other n-phase IMs.

Acknowledgment

The authors wish to thank the financial support from the Paraguayan Science and Technology National Council (CONACYT) through project 14-INV-101 and the research stay grant PVCT 17-6.

References

[1] F. Barrero and M. J. Duran, "Recent advances in the design, modeling, and control of multiphase machines: Part I," *IEEE Trans. Ind. Electron.*, vol. 63, no. 1, pp. 449–458, 2016.

[2] M. J. Duran and F. Barrero, "Recent advances in the design, modeling, and control of multiphase machines: Part II," *IEEE Trans. Ind. Electron.*, vol. 63, no. 1, pp. 459–468, 2016.

[3] E. Levi, "Advances in converter control and innovative exploitation of additional degrees of freedom for multiphase machines," *IEEE Trans. Ind. Electron.*, vol. 63, no. 1, pp. 433–448, 2016.

[4] C. Lim, E. Levi, M. Jones, N. Rahim, and W. P. Hew, "FCS-MPC based current control of a five-phase induction motor and its comparison with PI-PWM control," *IEEE Trans. Ind. Electron.*, vol. 61, no. 1, pp. 149–163, 2014.

[5] J. A. Riveros, F. Barrero, E. Levi, M. J. Duran, S. Toral, and M. Jones, "Variable-speed five-phase induction motor drive based on predictive torque control," *IEEE Trans. Ind. Electron.*, vol. 60, no. 8, pp. 2957–2968, 2013.

[6] J. Rodas, F. Barrero, M. R. Arahal, C. Martín, and R. Gregor, "Online estimation of rotor variables in predictive current controllers: a case study using five-phase induction machines," *IEEE Trans. Ind. Electron.*, vol. 63, no. 9, pp. 5348–5356, 2016.

[7] A. Taheri, A. Rahmati, and S. Kaboli, "Efficiency improvement in DTC of six-phase induction machine by adaptive gradient descent of flux," *IEEE Trans. Power Electron.*, vol. 27, no. 3, pp. 1552–1562, 2012.

[8] A. G. Yepes, J. Malvar, A. Vidal, O. López, and J. Doval-Gandoy, "Current harmonics compensation based on multiresonant control in synchronous frames for symmetrical n-phase machines," *IEEE Trans. Ind. Electron.*, vol. 62, no. 5, pp. 2708–2720, 2015.

[9] R. Gregor and J. Rodas, "Speed sensorless control of dual three-phase induction machine based on a Luenberger observer for rotor current estimation," in *Proc. IECON*, pp. 3653–3658, 2012.

[10] M. Ayala, O. Gonzalez, J. Rodas, R. Gregor, and J. Doval-Gandoy, "A speed-sensorless predictive current control of multiphase induction machines using a Kalman filter for rotor current estimator," in *Proc. ESARS-ITEC*, pp. 1–6, 2016.

[11] H. Guzman, M. J. Duran, F. Barrero, L. Zarri, B. Bogado, I. G. Prieto, and M. R. Arahal, "Comparative study of predictive and resonant controllers in fault-tolerant five-phase induction motor drives," *IEEE Trans. Ind. Electron.*, vol. 63, no. 1, pp. 606–617, 2016.

[12] M. Bermudez, I. Gonzalez-Prieto, F. Barrero, H. Guzman, M. J. Duran, and X. Kestelyn, "Open-phase fault-tolerant direct torque control technique for five-phase induction motor drives," *IEEE Trans. Ind. Electron.*, vol. 64, no. 2, pp. 902–911, 2017.

[13] F. Baneira, J. Doval-Gandoy, A. G. Yepes, O. López, and D. Pérez-Estévez, "Control strategy for multiphase drives with minimum losses in the full torque operation range under single open-phase fault," *IEEE Trans. Power Electron.*, vol. 32, no. 8, pp. 6275–6285, 2017.

[14] J. Rodas, H. Guzman, R. Gregor, and B. Barrero, "Model predictive current controller using Kalman filter for fault-tolerant five-phase wind energy conversion systems," in *Proc. PEDG*, pp. 1–6, 2016.

[15] M. A. Fnaiech, F. Betin, G.-A. Capolino, and F. Fnaiech, "Fuzzy logic and sliding-mode controls applied to six-phase induction machine with open phases," *IEEE Trans. Ind. Electron.*, vol. 57, no. 1, pp. 354–364, 2010.

[16] V. Utkin, J. Guldner, and J. Shi, *Sliding mode control in electromechanical systems*. Taylor-Francis, 1999.

[17] L. Fridman, "An averaging approach to chattering," *IEEE Trans. Autom. Control*, vol. 46, pp. 1260–1265, 2001.

[18] I. Boiko and L. Fridman, "Analysis of chattering in continuous sliding-mode controllers," *IEEE Trans. Autom. Control*, vol. 50, pp. 1442–1446, 2005.

[19] A. Levant, "Sliding order and sliding accuracy in sliding mode control," *Int. J. Control*, vol. 58, no. 6, pp. 1247–1263, 1993.

[20] L. Fridman and A. Levant, "Higher order sliding mode," in *Systems and Control Book Series*, 2002.

[21] G. Bartolini, A. Pisano, E. Punta, and E. Usai, "A survey of applications of second-order sliding mode control to mechanical systems," *Int. J. Control*, vol. 76, no. 9-10, pp. 875–892, 2003.

[22] Y. Shtessel, C. Edwards, L. Fridman, and A. Levant, *Sliding Mode Control and Observation*. Springer, New York, 2014.

[23] V. Utkin, "On convergence time and disturbance rejection of super-twisting control," *IEEE Trans. Autom. Control*, vol. 58, pp. 2013–2017, August 2013.

[24] E. Guzmán and J. A. Moreno, "Super-twisting observer for second-order systems with time-varying coefficient," *IET Control Theory Appl.*, vol. 9, no. 4, pp. 553–562, 2015.

[25] K. Youcef-Toumi and O. Ito, "A time delay controller for systems with unknown dynamics," *ASME J. Dyn. Syst. Meas. Control*, vol. 112, pp. 133–141, 1990.

[26] T. Hsia and L. Gao, "Robot manipulator control using decentralized linear time-invariant time-delayed joint controllers," *Proc. ICRA*, vol. 3, pp. 2070–2075, 1990.

[27] Y. Kali, M. Saad, K. Benjelloun, and M. Benbrahim, "Sliding mode with time delay control for MIMO nonlinear systems with unknown dynamics," in *Proc. RASM*, pp. 1–6, 2015.

[28] J. A. Moreno and M. Osorio, "A Lyapunov approach to second-order sliding mode controllers and observers," in *Proc. CDC*, pp. 2856–2861, 2008.

[29] E. Kreindler and E. Jameson, "Conditions for nonnegativeness of partioned matrices," *IEEE Trans. Autom. Control*, vol. 17, no. 1, pp. 147 – 148, 1972.